Canadian Science Publishing
NRC Research Press journals | Publishing Services

Canadian Journal of Chemistry
Revue canadienne de chimie

Pharmacophore modeling and molecular docking studies of acridines as potential DPP-IV inhibitors

Journal:	*Canadian Journal of Chemistry*
Manuscript ID:	Draft
Manuscript Type:	Article
Date Submitted by the Author:	n/a
Complete List of Authors:	Abu Khalaf, Reema; Al-Zaytoonah University of Jordan, pharmacy Jarekji, Zainab; Al-Zaytoonah University of Jordan, Pharmacy Al-Qirim, Tariq; Al-Zaytoonah University of Jordan, Pharmacy Sabbah, Dima; Al-Zaytoonah University of Jordan, Pharmacy Shatat, Ghassan; Al-Zaytoonah University of Jordan, Pharmacy
Keyword:	Acridines, Diabetes, Docking, DPP-IV Inhibitors, Pharmacophore modeling

Pharmacophore modeling and molecular docking studies of acridines as potential DPP-IV inhibitors

R. Abu Khalaf, Z. Jarekji, T. Al-Qirim, D. Sabbah, G. Shatat

R. Abu Khalaf,[1] Z. Jarekji, T. Al-Qirim, D. Sabbah, G. Shatat

Department of Pharmacy, Faculty of Pharmacy, Al-Zaytoonah University of Jordan, Amman, Jordan.

[1]Corresponding author address: Department of Pharmacy, Faculty of Pharmacy, Al-Zaytoonah University of Jordan, Amman, Jordan; Telephone: 00962 6 4291511; Ext 239; Fax: 00962 6 4291432; E-mail: reema.abukhalaf@zuj.edu.jo or rima_abu_khalaf@yahoo.com

Abstract:

Inhibition of dipeptidyl peptidase-IV (DPP-IV) prevents the inactivation of gastric inhibitory polypeptide (GIP) and glucagon like peptide-1 (GLP-1). This increases circulating levels of active GLP-1 and GIP, stimulates insulin secretion, which results in lowering of glucose levels and improvement of the glycemic control in patients with type 2 diabetes.

In this study, pharmacophore modeling and docking experiments were carried out and a series of 8 novel 2-ethoxy-6, 9-disubstituted acridines (**13, 15, 17a-17f**) have been designed and synthesized. Then these compounds were evaluated for their ability to inhibit DPP-IV. Most of the synthesized compounds were proved to have anti-DPP-IV activity where compound **17b** displayed the best activity of 43.8 % inhibition at 30 μM concentration. Results of this work might be helpful for further optimization to develop more potent DPP-IV inhibitors.

Key words:

Acridines, Diabetes, Docking, DPP-IV Inhibitors, Pharmacophore modeling.

Introduction

Diabetes is a chronic disease that occurs either when the pancreas does not produce enough insulin or when the body cannot effectively use the insulin it produces.[1] Hyperglycemia is a common effect of uncontrolled diabetes and over time leads to serious damage to many of the body's systems, especially the nerves and blood vessels.[2] Most cases of diabetes mellitus fall into the three broad categories of type 1 or insulin dependent diabetes mellitus, type 2 or noninsulin dependent diabetes mellitus and gestational diabetes mellitus.[2]

It has long been shown that hormones of the gastrointestinal system can modulate the secretory activities of the islets of Langerhans. They were referred to as incretins.[3] The first set of biologically active incretins to be identified was the gastric inhibitory polypeptide (GIP).[4] Glucagon-like peptide-1 (GLP-1) was recognized to have a potent insulinotropic activity.[3]

GIP and GLP-1 are quickly deactivated by dipeptidyl peptidase-IV (DPP-IV).[4,5] DPP-IV, can cleave the active peptide at position 2 alanine (*N*-terminal) resulting in an inactive compound.[6]

DPP-IV is a large, 766 amino acid membrane-associated, serine-type protease enzyme.[7] The enzyme is widely detected in numerous tissues such as kidney, liver, intestine, spleen, lymphocytic organs, placenta, adrenal glands, and vascular endothelium.[8] DPP-IV is arranged in two domains: an *N*-terminal β-propeller domain and a *C*-terminal α/β-hydrolase domain. The two domains form a large cavity that houses the active site.[9]

Access to the active site, is via an opening in the centre of the β-propeller or through the larger opening between the propeller and hydrolase domains.[10] Several residues were

found to be essential to the catalytic activity of DPP-IV such as Ser630, His740, Tyr547, Glu205 and Glu206.[11,12]

Recently, a variety of DPP-IV inhibitor classes have been developed. These DPP-IV inhibitors comprise different scaffolds and ring systems, such as sulfonamides,[13] purines,[14-18] xanthenes,[19-23] quinolines,[24-26] tricyclic[27-29] and tetracyclic ring systems[30] (Fig. 1a).

None of the earlier efforts to develop new DPP-IV inhibitors used the tricyclic acridine ring as a chief scaffold. Subsequently, this encourages us to synthesize and biologically evaluate this novel series of compounds as potential DPP-IV inhibitors (Fig. 1b).

Fig. 1. (a) Chemical scaffolds of previously reported DPP-IV inhibitors compared to **(b)** the synthesized 2-ethoxy-6, 9-disubstituted acridine-based DPP-IV inhibitors.

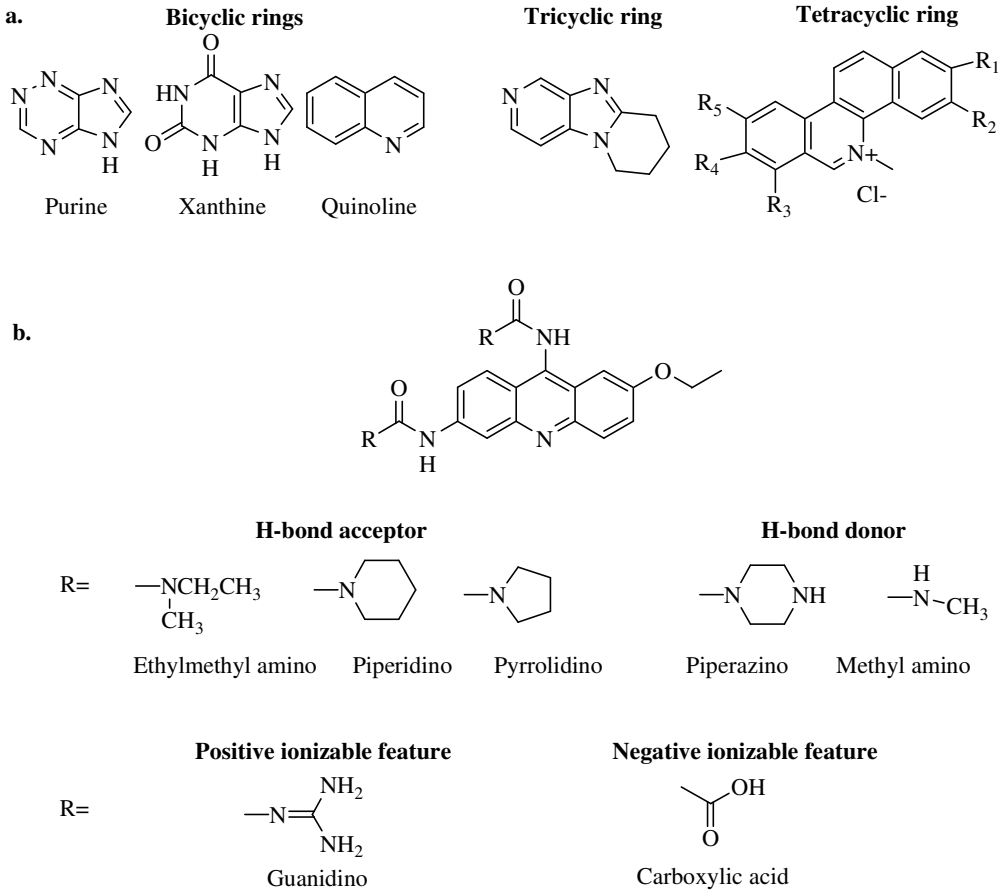

Experimental

Computational methods:

Preparation of protein structure

The coordinates of native DPP-IV (PDB id: 4A5S)[31] with no missing residues was prepared using the Protein Preparation wizard in the Schrödinger software[32] suite to maximize H-bond interactions.

Preparation of ligand structures

The ligands (**1-10**)[31, 33-36] were built based on the coordinates of crystallized ligand in 4A5S. The ligands were built using MOE build panel and subsequently prepared using ligprep module in Maestro.

Induced-fit docking (IFD)

The ligand was defined as a centroid in the peptidase binding cleft. Both enzyme and ligand Vander Waals scaling factors were set to 0.5 to allow enough flexibility for the best docked ligand pose. Other settings were determined as default. The ligand pose with the highest XP Glide score was reported.

Chemistry:

Materials and instruments

All chemicals, reagents and solvents were of analytical grade and used directly without further purification. Chemicals and solvents were purchased from corresponding companies (Sigma-Aldrich, Acros, Tiedia, fisher chemical, laboratory Rasayan).

6, 9-Diamino-2-ethoxyacridine lactate monohydrate, bromo acetyl chloride, propanoic acid-3-chloro-3-oxoethyl ester, acetic acid-2-chloro-2-oxoethyl ester, methanamine,

guanidine.HCl, pyrrolidine, piperazine, piperidine and *N*-methylethanamine were purchased from Acros ltd. through local agent.

Rotavapour model R-114 purchased from Buchi, Switzerland. Melting points were measured using Gallenkamp melting point apparatus, and are uncorrected. Infrared spectra were recorded using Shimadzu IR Affinity-1 spectrophotometer. All samples were prepared as potassium bromide (Acros, Belgium) discs. ^{1}H- and ^{13}C-NMR spectra were measured using Bruker 500 MHz (Avance III, Switzerland Department of chemistry, University of Jordan). Deuterated solvents were used and stated with each compound.

Thin Layer Chromatography (TLC) was performed on 20 x 20 cm aluminum plates pre-coated with fluorescent silica gel GF254 (Macherey-Nagel, Germany), and visualized by UV light (at 254 and/ or 360 nm). Column chromatography was carried out using high-purity grade silica gel as stationary phase, pore size 60 A°, 70-230 mesh , 63-200 µm (Sigma aldrich).

Synthesis of the required compounds

N-[2-Ethoxy-6-(oxalyl-amino)-acridin-9-yl]-oxalamic acid (13)

A solution of 7-ethoxyacridine-3,9-diamine **11** (0.5 g, 1.38 mmole) in toluene (50 ml) was stirred at room temperature, and then a dropwise addition of acetic acid-2-chloro-2-oxoethyl ester (0.45 ml, 4.14 mmole) was carried out followed by 5 drops of ammonia. Subsequently, the reaction was refluxed overnight.[37] The residue after evaporation of the solvent was purified by column chromatography eluting with (chloroform/ethanol, 85:15) to give intermediate **12** as a yellow solid (0.56 g, 90.2%). Mp. decomposed over 250°C,

R_f = 0.62 (chloroform/methanol, 80:20). IR (KBr disc): 1203, 1497, 1589, 1674, 1751, 3117 cm^{-1}.

Afterward, a mixture of **12** (0.4 g, 0.88 mmole) and 6 ml of 4M NaOH was stirred in methanol at room temperature overnight. Then the reaction mixture was neutralized with diluted HCl and then filtered to give the title compound **13** as a yellow solid (0.15 g, 44%). Mp. decomposed over 250°C, R_f =0.72 (chloroform/methanol, 90:10), ^{1}H-NMR (500 MHz, DMSO-d*6*): δ 1.42 (t, *J*=7 Hz, 3H, OCH_2CH_3), 4.17 (q, *J*=7 Hz, 2H, OCH_2CH_3), 6.65 (d, *J*=8.5 Hz, 1H, Ar), 7.62 (dd, *J*=2.4, 0.1 Hz, 1H, Ar), 7.66 (d, *J*=8.5 Hz, 1H, Ar), 7.75 (dd, *J*=1.7, 0.1 Hz , 1H, Ar), 7.86 (d, *J*=9.3 Hz, 1H, Ar), 8.06 (br s, 1H, CONH), 8.33 (br s, 1H, CONH), 8.69 (d, *J*=9.3 Hz, 1H, Ar), 11.35 (s, 1H, COOH), 13.77 (s, 1H, COOH) ppm; ^{13}C-NMR (DMSO-d*6*): δ = 51.7 (1C), 64.6 (1C), 104.3 (1C), 106.7 (1C), 108.3 (1C), 112.9 (1C), 118.0 (1C), 120.8 (1C), 126.1 (1C), 128.1 (1C), 131.5 (1C), 135.4 (1C), 140.0 (1C), 143.3 (1C), 155.3 (1C), 156.0 (1C), 158.4 (1C), 161.9 (1C), 166.7 (1C) ppm; IR (KBr disc): 1204, 1497, 1667, 1785, 2994, 3132, 3294, 3395 cm^{-1}.

N-[6-(2-Carboxy-acetylamino)-2-ethoxy-acridin-9-yl]-malonamic acid (15)

A suspension of 7-ethoxyacridine-3,9-diamine **11** (0.5 g, 1.38 mmole) in propanoic acid-3-chloro-3-oxoethyl ester (10 ml, 78.11 mmole) was stirred for 1hr at room temperature, then the temperature was raised to 90°C for another 1hr and finally the reaction mixture was refluxed for 6hrs. Afterward, it was allowed to stand at room temperature overnight and then chilled with ice-water. The product was collected and washed with acetone (10 ml), toluene (10 ml), acetone again (10 ml), ethanol (10 ml), ether (10 ml) and finally hexane (10 ml).[38] The product was dried over calcium sulfate under vacuum to yield intermediate **14** as a brown powder (0.23 g, 35.9%). Mp. decomposed over 250°C, R_f =

0.6 (chloroform/methanol, 80:20), IR (KBr disc):1497, 1636, 1667, 1736, 2932, 3210, 3526 cm^{-1}.

A mixture of **14** (0.2 g, 0.43 mmole) and 6 ml of 4M NaOH was stirred in methanol-THF (1:4) at room temperature overnight. Then the solvent was evaporated and the residue was diluted with water, followed by neutralizing the reaction mixture with HCl and filtration to yield the title compound **15** as a yellow solid (0.12 g, 66.6%). Mp. decomposed over 250°C, R_f = 0.7 (chloroform/methanol, 70:30), ^{1}H-NMR (500 MHz, DMSO-d*6*): δ 1.40 (t, *J*=4 Hz, 3H, OCH_2CH_3), 3.09 (s, 2H, $COCH_2CO$), 3.17 (s, 2H, $COCH_2CO$), 4.19 (q, *J* =4 Hz, 2H, OCH_2CH_3), 6.82 (s, 1H, Ar), 7.40 (d, *J*=8.5 Hz, 1H, Ar), 7.49 (d, *J*=8 Hz, 1H, Ar), 7.76 (d, *J*=8.5 Hz, 1H, Ar), 7.82 (s, 1H, Ar), 7.99 (s, 1H, CONH), 8.28 (s, 1H, CONH), 8.36 (d, *J*=8 Hz, 1H, Ar), 9.17 (s, 1H, COOH), 12.23 (s, 1H, COOH) ppm; ^{13}C-NMR (DMSO-d*6*): δ = 15.1 (1C), 46.3 (1C), 64.2 (1C), 64.5 (1C), 102.7 (1C), 103.5 (1C), 104.8 (1C), 108.9 (1C), 112.3 (1C), 113.0 (1C), 116.3 (1C), 117.1 (1C), 120.3 (1C), 124.9 (1C), 126.0 (1C), 126.2 (1C), 126.5(1C), 154.4 (1C), 155.0 (1C), 171.2 (1C), 172.2 (1C) ppm; IR (KBr disc): 1041, 1165, 1242, 1381, 1497, 1597, 1636, 1790, 2924, 3217, 3418 cm^{-1}.

General procedure for the synthesis of N-[2-ethoxy-6-(2-(substituted-amino-acetylamino)-acridin-9-yl]-2-(substituted-amino)-acetamide (17a-17f)

A solution of 7-ethoxyacridine-3,9-diamine **11** (2 g, 5.5 mmole) in toluene (50 ml) was stirred at room temperature, and then a dropwise addition of bromo acetyl chloride (2.29 ml, 27 mmole) was carried out followed by the addition of 0.3 ml ammonia and the reaction was refluxed overnight**.** Subsequently, the solvent was evaporated to yield intermediate **16** as a yellow solid (2.64 g, 97.7%). Mp. decomposed over 250°C, R_f =

0.54 (chloroform/ methanol, 80:20), IR (thin film): 1404, 1497, 1558, 1597, 1659, 2978, 3179, 3395 cm^{-1}.

Afterward, intermediate **16** (0.5 g, 1 mmole) and NaI (0.1g) were suspended in a mixture of DMF (7.5 ml) and ethanol (7.5 ml) followed by the addition of one of the substituted amines (methanamine, *N*-methylethanamine, pyrrolidine, piperazine, piperidine and guanidine). Then, the reaction mixture was refluxed for 24hr. Subsequently, the reaction mixture was cooled and the solvent was evaporated under reduced pressure. The residue was washed with DMF (20 ml). The process was repeated using toluene (2×15ml) and propan-2-ol (2×15ml). Later, the solid residue was dissolved in water and the final product was precipitated out using ammonia.[38]

N-[2-Ethoxy-6-(2-methylamino-acetylamino)-acridin-9-yl]-2-methylamino-acetoamide (17a)

Intermediate **16** was reacted with methylamine (0.943 g, 1.2 ml, 30 mmole) according to the above general procedure. The collected filtrate was purified by column chromatography (methanol: 3drop ammonia) to yield **17a** as a dark yellow liquid (0.183 g, 49.4%), R_f = 0.24 (methanol: 10 drops ammonia). ^{1}H-NMR (500 MHz, DMSO-d*6*): δ= 1.18 (d, *J*=6.65 Hz, 6H, NHC*H*$_3$), 1.43 (t, *J*=6.9 Hz, 3H, OCH$_2$*CH*$_3$), 3.63 (s, 4H, NC*H*$_2$CO), 3.79 (q, *J*=6.6 Hz, 2H, O*CH*$_2$CH$_3$), 5.77 (br s, 2H, *NH*CH$_3$), 7.51 (d, *J*=8.25 Hz, 1H, Ar), 7.57 (d, *J*=9 Hz, 1H, Ar), 7.68-7.3 (m, 2H, Ar), 8.42 (s, 1H, Ar), 8.44 (d, *J*=8.5 Hz, 1H, Ar), 8.42 (s, 1H, CON*H*), 10.17 (s, 1H, CON*H*) ppm; ^{13}C-NMR (DMSO-d*6*): δ = 15.0 (1C), 24.6 (1C), 39.3 (1C), 49.1 (1C), 61.7 (1C), 67.5 (1C), 102.7 (1C), 106.2 (1C), 109.9 (1C), 113.0 (1C), 117.2 (1C), 124.8 (1C), 129.1 (1C), 132.1 (1C), 139.6 (1C), 145.3 (1C), 147.8 (1C), 154.0 (1C), 161.2 (1C), 176.0 (1C), 178.6 (1C) ppm;

IR (KBr disc): 1042 ,1080 ,1126 ,1242 ,1311, 1412, 1466, 1589, 1728, 2924, 2978, 3426, 3580 cm^{-1}.

N-{2-Ethoxy-6-[2-(ethyl-methyl-amino)-acetylamino]-acridin-9-yl}-2-(ethyl-methyl-amino)-acetamide (17b)

Intermediate **16** was reacted with *N*-ethyl methyl amine (1.77 g, 2.6 ml, 30 mmole) according to the above general procedure. The collected precipitate was purified by column chromatography methanol: 3 drop ammonia to yield **17b** as a dark yellow solid (0.275 g, 60.9%), Mp. decomposed over 260°C , R_f = 0.31 (methanol:10 drop ammonia). ^{1}H-NMR (500 MHz, DMSO-d*6*): δ= 1.13 (t, *J*=7.2 Hz, 6H, NCH_2CH_3), 1.43 (t, *J*=6.9 Hz, 3H, OCH_2CH_3), 2.65 (s, 6H, NCH_3), 2.92 (q, *J*=7.2 Hz, 4H, NCH_2CH_3), 3.26 (s, 4H, NCH_2CO), 4.19 (q, *J*=6.9 Hz, 2H, OCH_2CH_3), 7.3 (dd, *J*=1.9, 9 Hz, 1H, Ar), 7.55 (dd, *J*=1.9, 9 Hz, 1H, Ar), 7.79 (s, 1H, Ar), 7.80 (d, *J*=9 Hz, 2H, Ar), 8.40 (s, 1H, Ar), 8.42 (s, 1H, CON*H*), 10.17 (s, 1H, CON*H*) ppm; ^{13}C-NMR (DMSO-d*6*): δ = 10.4 (1C), 12.6 (1C), 15.1 (1C), 21.5 (1C), 50.9 (1C), 51.5 (1C), 58.74 (1C), 61.5 (1C), 64.2 (1C), 102.7 (1C), 106.2 (1C), 109.9 (1C), 113.0 (1C), 117.2 (1C), 124.8 (1C), 129.1 (1C), 132.1 (1C), 139.6 (1C), 145.3 (1C), 147.8 (1C), 154.0 (1C), 161.2 (1C), 167.3 (1C), 170.5 (2C) ppm; IR (KBr disc): 1111, 1366, 1466, 1512, 1543, 1636, 2924, 3449, 3564 cm^{-1}.

N-[2-Ethoxy-6-(2-piperazine-1-yl-acetylamino)-acridin-9-yl]-2-piperazine-1-acetamide (17c)

Intermediate **16** was reacted with piperazine (2.58 g, 30 mmole) according to the above general procedure. The collected filtrate was purified by column chromatography (methanol: 3drop ammonia) to yield **17c** as a dark yellow solid (0.260 g, 51.4%), Mp. decomposed over 260°C, R_f = 0.3 (methanol: 10 drop ammonia), ^{1}H-NMR (500 MHz, DMSO-d*6*): δ=1.43 (t, *J*=7 Hz, 2H, OCH_2CH_3), 2.37 (t, *J*=5 Hz, 8H, piperazine), 2.43 (t,

J=5 Hz, 4H, piperazine), 2.60 (t, *J*=5 Hz, 4H, piperazine), 2.81 (s, 2H, NC*H*$_2$CO), 3.13 (s, 2H, NC*H*$_2$CO), 3.75 (br s, 2H, *H*N-piperazine), 4.18 (q, *J*=7 Hz, 2H, OC*H*$_2$CH$_3$), 7.34 (dd, *J*=9.2 Hz, 1H, Ar), 7.51 (dd, *J*=9 , 2 Hz, 1H, Ar), 7.73 (d, *J*=9 Hz, 1H, Ar), 7.97 (s, 1H, Ar), 8.03 (s, 1H, Ar), 8.30 (d, *J*=9 Hz, 1H, Ar), 8.50 (s, 1H, CON*H*), 10.02 (s, 1H, CON*H*) ppm; ^{13}C-NMR (DMSO-d*6*): δ = 15.1 (1C), 52.2 (1C), 52.5 (1C), 53.4 (1C), 53.7 (1C), 53.8 (1C), 54.2 (1C), 60.4 (1C), 60.5 (1C), 62.0 (1C), 62.4 (1C), 64.0 (1C), 101.7 (1C), 106.2 (1C), 110.0 (1C), 113.2 (1C), 117.2 (1C), 124.1 (1C), 124.4 (1C), 129.8 (1C), 139.6 (1C), 145.3 (1C), 148.0 (1C), 148.1 (1C), 153.8 (1C), 167.5 (1C), 171.5 (1C) ppm; IR (KBr disc): 1011, 1042, 1119, 1219 , 1450, 1651, 2932, 3024, 3356, 3456, 3564 cm^{-1}.

N-[2-Ethoxy-6-(2-pyrrolidin-1-yl-acetylamino)-acridin-9-yl]-2-pyrrolidin-1-yl-acetamide (17d)

Intermediate **16** was reacted with pyrrolidine (2.13 g, 2.4 ml, and 30 mmole) according to the above general procedure. The collected precipitate was purified by column chromatography (methanol: 3drop) ammonia to yield **17d** as a dark yellow solid (0.302 mg, 63.6%), Mp. decomposed over 270°C, R$_f$ = 0.18 (methanol: 10 drop ammonia), ^{1}H-NMR (500 MHz, MeOD): δ=1.49 (t, *J*=6.9 Hz, 3H, OCH$_2$C*H*$_3$), 3.02 (s, 4H, C*H*$_2$CONH), 3.40 (t, *J*=6.3 Hz, 8H, pyrrolidine), 3.58 (t, *J*=6.3 Hz, 8H, pyrrolidine), 4.15 (q, *J*=6.9 Hz, 2H, OC*H*$_2$CH$_3$), 7.31-7.73 (m, 6H, Ar), 8.21 (s, 1H, CON*H*), 8.43 (s, 1H, CON*H*) ppm; ^{13}C-NMR (MeOD): δ = 23.1 (1C), 23.7 (4C), 43.0 (4C), 46.2 (1C), 54.2 (1C), 102.2 (1C), 105.2 (1C), 107.5 (1C), 112.4 (1C), 117.2 (1C), 119.0 (1C), 119.8 (1C), 124.7 (1C), 125.0 (1C), 126.2 (1C), 127.9 (1C), 128.3 (1C), 140.0 (1C), 143.7 (1C),

155.8 (1C), 161.8 (1C) ppm; IR (KBr disc): 1042, 1111, 1227, 1396, 1474, 1528, 1674, 2970, 3210, 3325 cm^{-1}.

N-[2-Ethoxy-6-(2-piperidin-1-yl-acetylamino)-acridin-9-yl]-2-piperidin-1-acetamide (17e)

Intermediate **16** was reacted with piperidine (2.55 g, 2.96 ml, 30 mmole) according to the above general procedure. The collected precipitate was purified by column chromatography (chloroform/methanol, 80:20) to yield **17e** as a dark yellow solid (0.312 mg, 62%), Mp. decomposed over 260°C, R_f=0.5 (chloroform/methanol, 80:20), ^{1}H-NMR (500 MHz, DMSO-d*6*): δ= 0.86 (t, *J*=7 Hz, 3H, OCH_2CH_3), 1.08-1.4 (m, 20H, piperidine), 1.55 (s, 2H, $COCH_2$), 2.46 (s, 2H, $COCH_2$), 4.13 (q, *J*=7 Hz , 2H, OCH_2CH_3), 8.26-7.26 (m, 6H, Ar), 8.18 (s, 1H, CONH), 8.25 (s, 1H, CONH) ppm; ^{13}C-NMR (DMSO-d*6*): δ = 14.4 (1C), 22.0 (2C), 24.0 (2C), 26.0 (2C), 29.2 (2C), 29.5 (2C), 54.6 (1C), 67.9 (2C), 101.7 (1C), 110.0 (1C), 113.3 (1C), 115.2 (1C), 117.1 (1C), 124.1 (1C), 124.3 (1C), 129.2 (1C), 130.2 (1C), 132.2 (1C), 139.4 (1C), 148.7 (1C), 153.8 (1C), 167.5 (1C), 170.0 (1C) ppm; IR (KBr disc): 1018, 1219, 1443, 1497, 1612, 1721, 2932, 3117, 3410, 3487 cm^{-1}.

N-[2-Ethoxy-6-(2-guanidino-acetylamino)-acridin-9-yl]-2-guanidino-acetamide (17f)

Ethylamine (4 ml) was added to guanidine.HCl (2.75 g, 30 mmole) then added to intermediate **16** according to the above general procedure. The collected precipitate was purified by column chromatography (methanol: 3drop ammonia) to yield yellow solid (0.313 mg, 60.4%). Mp. decomposed over 250°C, R_f = 0.31 (methanol: 10 drop ammonia).^{1}H-NMR (500 MHz, DMSO-d*6*): δ=1.15 (t, *J*=7 Hz, 3H, OCH_2CH_3), 3.36 (br s, 8H, $N=CNH_2$), 3.43 (s, 4H, NCH_2CO), 3.49 (q, *J*=7 Hz, 2H, OCH_2CH_3), 7.37 (d, *J*=8.7 Hz, 1H, Ar), 7.56 (d, *J*=9 Hz, 1H, Ar), 7.68-7.75 (m, 2H, Ar), 8.31 (s, 1H, Ar), 8.35 (d,

J=8.7 Hz, Ar), 8.48 (br s, 1H, CON*H*), 10.10 (br s, 1H, CON*H*) ppm; ^{13}C-NMR (DMSO-d*6*): δ =14.4 (1C), 22.9 (1C), 29.4 (1C), 67.9 (1C), 102.7 (1C), 106.2 (1C), 109.9 (1C), 113.0 (1C), 117.2 (1C), 124.8 (1C), 129.1 (1C), 130.1 (1C), 132.1 (1C), 139.6 (1C), 145.3 (1C), 147.8 (1C), 148.7 (1C), 154.0 (1C), 161.2 (1C), 164.8 (1C), 165.1 (1C) ppm; IR (KBr disc): 1165, 1242, 1396, 1466, 1543, 1612, 1744, 2924, 3148, 3287 cm^{-1}.

DPP-IV inhibition assay:

DPP-IV inhibitory bioactivities were assayed by fluorescence-based commercially available kit (Cayman Chemical Company, Ann Arbor, USA). The assay kit is based on fluorogenic substrate, Gly-Pro-Aminomethyl coumarin (AMC). Cleavage of the peptide bond by DPP-IV releases the free AMC group resulting in fluorescence. Inhibition of DPP-IV will prevent cleavage of the peptide and therefore decrease fluorescence intensity.

The assay procedure can be described briefly as follows: 30 µl of the provided assay buffer, 10 µl of tested inhibitor and 10 µl of diluted DPP-IV were added to the inhibitor wells. The reaction was initiated by adding 50 µl of diluted substrate solution. The plate was covered and incubated for 30 minutes at 37 °C. After incubation, fluorescence intensity (Excitation λ: 350 nm; Emission λ: 465 nm) was read in a FLX800TBI Microplate Fluorimeter (BioTek Instruments, Winooski, USA). The assay is carried out using a black 96-well plate with led.

The tested compounds were initially dissolved in DMSO to yield 10 mM stock solutions and subsequently diluted to the required concentrations using distilled water and then were added to the assay well in a final volume of 10 µl (and a final concentration of 30 µM). The final concentration of DMSO was adjusted to 0.1 %. The percentage of residual

activity of DPP-IV was determined for each compound by comparing the activity of DPP-IV in the presence and absence of the tested compound. Gemifloxacin was used as a positive control. DPP-IV was not affected by DMSO. Negative controls lacking human recombinant DPP-IV were used as background. All measurements were conducted in duplicates.[13]

Results and discussion

Generation of the pharmacophore model:

We adopted the coordinates of ligand **1** in PDB 4A5S[31] to build the 3D-sturctures of the reported DPP-IV inhibitors (**1-10**)[31, 33-36] (Fig. 2). Superposing the built compounds against the most potent inhibitor **2**[31] generated a pharmacophore model with the following features (Fig. 3). F1: one aromatic or heterocyclic or hydrophobic or H-bond acceptor or H-bond donor, F2: one heterocyclic or H-bond acceptor or H-bond donor, F3: one aromatic or hydrophobic or H-bond acceptor, F4: one hydrophobic or H-bond acceptor, F5: one aromatic or hydrophobic or H-bond acceptor.

Fig. 2. Structures of DPP-IV inhibitors (**1-10**) used in pharmacophore model building.

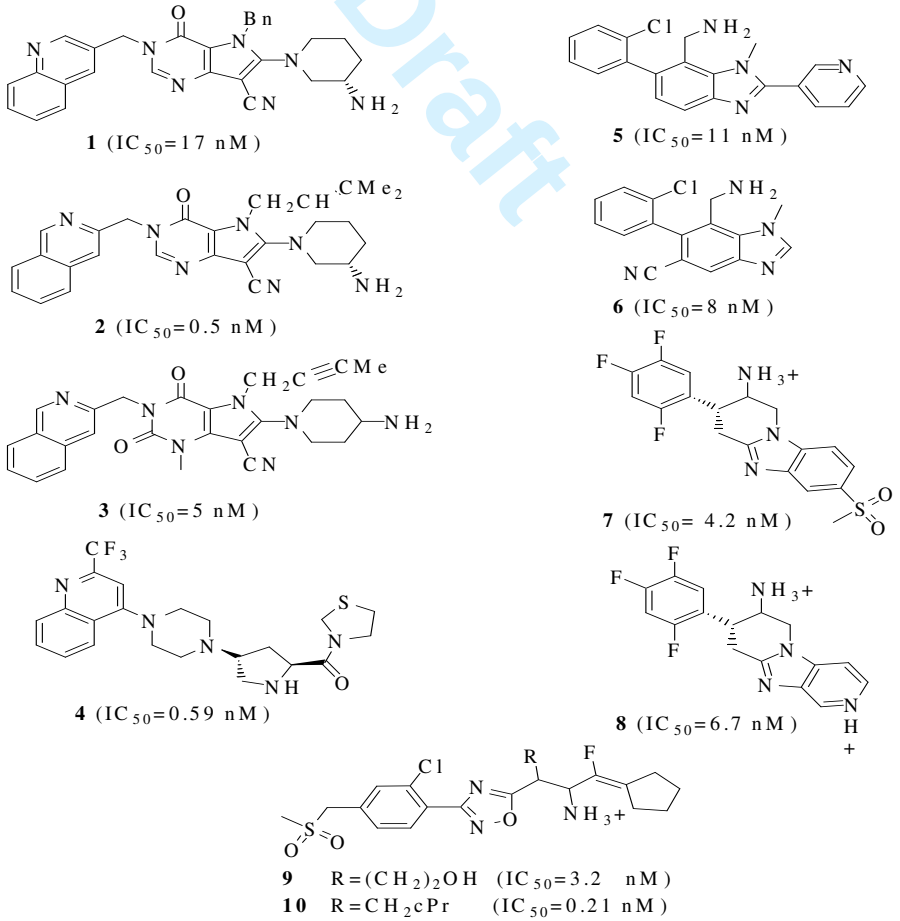

We found that the majority of DPP-IV inhibitors harbors a fused heterocyclic system; either a bicyclic or tricyclic ring. Surprisingly, the tricyclic acridine ring system has not been incorporated yet in the scaffold of DPP-IV inhibitors. Therefore, we suggested incorporating the acridine nucleus. We proposed a dataset of eight compounds having acridine scaffold tailored with different functionalities (**13, 15, 17a -17f**). In order to investigate if the prospective compounds satisfy the pharmacophore model, we searched the dataset against the generated model. Fortunately, our prospective compounds fit the five pharmacophoric points (Fig. S1, Supplementary data) and were reported as hits (Fig. 3).

Fig. 3. (a) The pharmacophoric point features of DPP-IV inhibitors. Aro stands for aromatic ring, Hyd: hydrophobic, Acc: acceptor, PIN: heterocyclic ring, Don: donor **(b)** and **(c)** pharmacophore model mapped with reported inhibitor **4** and the synthesized compound **17b**, respectively.

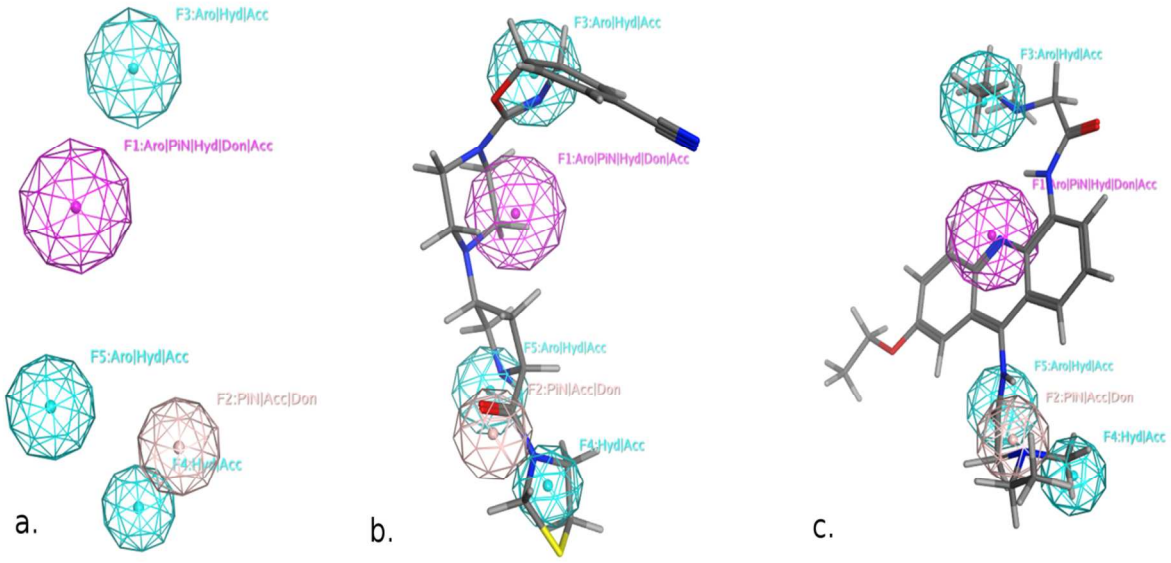

Molecular docking:

Validation of the induced fit docking (IFD)

The performance of the IFD program was evaluated by comparing the docked poses to native conformations in the crystal structures. The root mean square (rmsd) values for heavy atoms between the IFD-generated docked poses and the native poses for co-crystallized ligands (N7F, 317, 677, B2Y, 7AC, and W61) are listed in (Table 1). All docked poses have rmsd values lower than 2.0 Å.

Table 1. Ligand rmsd values (Heavy atoms, Å) between the IFD docked poses and the crystal structure native conformations.

Ligand	rmsd value
4A5S (N7F)	0.56
3C45 (317)	0.84
3HAB (677)	0.65
3CCB(B2Y)	0.13
3CCC(7AC)	0.14
3VJM(W61)	0.27

Figure 4 shows the superposition of the IFD-generated W61 and the native conformation in 3VJM, indicating that the IFD program is able to successfully reproduce the native conformation. The rmsd between these two poses is 0.27 Å. These low rmsd values indicate that IFD is capable to identify the native poses in crystal structures and can be reliably used to predict the binding conformations of other ligands.

Fig. 4. The superposition of the IFD generated pose and that of the crystal structure for 3VJM (W61). Hydrogen atoms are hidden for clarification. The superposed structure is represented in pink color. Picture made by PYMOL.

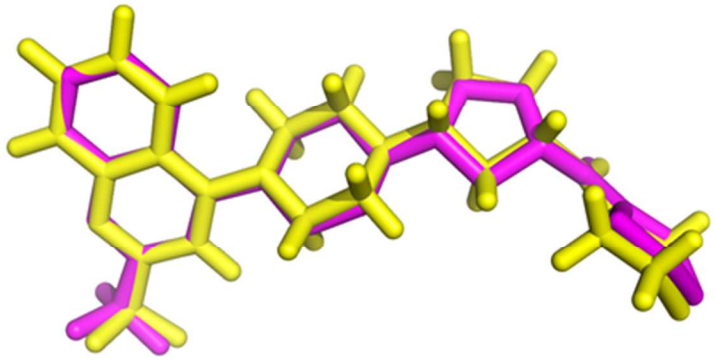

Binding mode of DPP-IV inhibitors

The active binding site of DPP-IV is defined as within 4.5 A° of the co-crystallized ligand (N7F) and it is enclosed by Arg125, Trp201, Glu204, Glu205, Glu206, Val207, Tyr256, Arg356, Phe357, Leu543, Leu544, Asp545, Val546, Tyr547, Ala548, Gly549, Pro550, Ser552, Lys554, Trp563, Ser577, Leu598, Trp627, Gly628, Trp629, Ser630, Tyr631, Gly632, Gly633, Tyr634, Val635, Thr636, Ile651, Val653, Ala654, Pro655, Val656, Trp659, Tyr662, Asp663, Tyr666, Thr667, Arg669, Tyr670, Asn710, Val711, Gln715, His740, Tyr752, Met755.

In order to determine the structural basis for binding of DPP-IV inhibitors, our verified compounds and the used compounds to build the pharmacophore model, we employed induced fit docking (IFD)[32,39] against the DPP-IV (4A5S). The IFD approach was proposed by Sherman *et al.*[40,41] and it takes into consideration the conformational changes in proteins. The IFD approach is processed by the following method: ligands are docked to a protein in a rigid docking using softened- potential docking with the Vander

Waals radii for protein atoms at a 0.7 scaling using the Glide program[32,42,43] and the top ligand poses are then subjected to a minimization along with protein residues within 5 Å of ligands using the Prime program,[32] followed by a redocking procedure against the minimized protein. In this way, protein plasticity can be taken into account during the whole docking process.

The IFD docking study shows that the verified compounds form H-bond with the backbones of Arg125, Glu205, Glu206, Ser209, Lys554, Tyr547, Asn562, Tyr585, Trp629, Ser630, Tyr631, Gly632, Tyr662, Asn710, Hid (His)740. The tightest binding to DPP-IV binding domain for the dataset is shown for the reported inhibitor **2** and our synthesized hit **17f** (Table 2). The flexibility and hydrophobic interaction of dimethyl propene moiety in **2** discusses its high binding affinity. The flexible chain is embedded in an aromatic groove consists of: Tyr631, Tyr634, Tyr659, Tyr662, and Tyr666. The closeness of the aromatic rings makes this groove tight and thus the flexible chain can only insert deeply in this domain. And, this clarifies the differences in binding affinity for compounds **1** and **3**. Compound **1** having the benzyl moiety forms π-stacking aromatic interaction with the aromatic residues. And, therefore the aromatic interaction enhances its binding affinity (Fig. 5a). Compound **3** misses one methyl group which contributes to lower binding affinity. This infers that flexible and branched chain having five carbons is favored to maximize binding interaction in the tight domain. It's worth noting that the size of the compound might contribute to good binding interaction if it accommodates properly the binding domain. Comparing compounds **6** and **7** shows that **6** has 3 rings while **7** owns 4 rings; the one ring difference could contributes to extra compound dimension that binds it to the backbones of key binding residues. And, therefore the

functionalities of **6** might be far away and thus no H-bond is formed. Though, we can't neglect the aromatic-π stacking which confers its binding affinity. The size of **4** and **5** and their functionalities are in accord with their binding affinities. Therefore, it is not surprisingly that **9** and **10** have distinct binding affinities.

Our synthesized compound **17f** having two guanidine moieties which provide strong ionic interaction with Glu206 and Asp545 (Table 2). And, the acridine scaffold contributes to aromatic-π stacking interaction with the aromatic residues. The strong positive charge of guanidine clarifies its tight binding compared to **17a**, **17b**, **17c**, **17d**, and **17e**. The steric hindrance of R might prohibit the ionic interaction as shown in **17b** which misses the ionic interaction with acidic residues. And, this explains its weakest binding affinity. Compounds **13** and **15** bearing acidic functionalities show significant interaction and this illustrate that ionic interaction with basic residues is required too. Compound **15** having extra methyl group which might shift it away from the counter residues to make ionic interaction. Thus, 1 Kcal/mol difference in binding emphasizes the length of the acidic attachment and might suggest that the shorter the R group holding acidic functionalities, the better the binder. Interestingly, gemifloxacin bearing both acidic and basic functionalities shows high affinity. It's worth noting that the –COOH moiety is directly attached to gemifloxacin's skeleton and this ensures that the length of acidic group is essential (Fig. 5b). Both acidic and basic functionalities furnish ionic interaction with the key binding residues. In addition to its size which occupies the binding domain and matches the stere of the tightest binder, these together explain the tight binding of gemifloxacin comparable to those of **2** and **17f**.

Fig. 5. Binding conformations of: **(a)** Inhibitor **1**, **(b)** gemifloxacin and **(c)** synthesized hit **17b** in the DPP-IV binding domains, H-bonds are depicted in dotted blue lines.

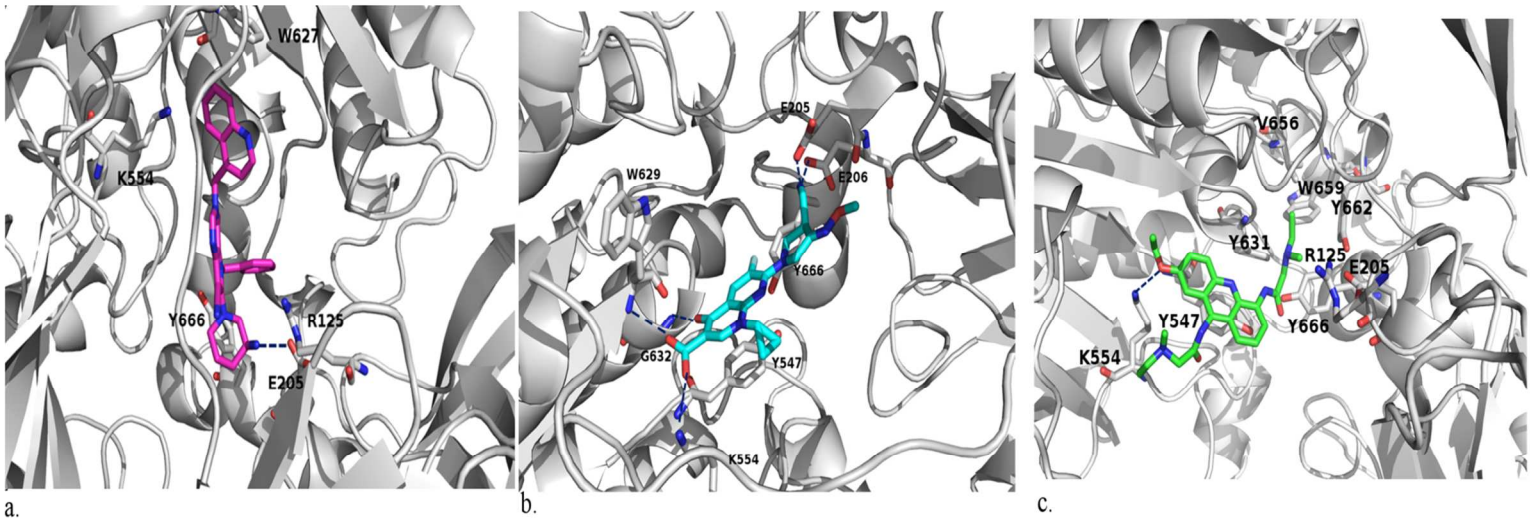

Comparing the % inhibition with the IFD docking score values show that the correlation factor R^2 ~0.51; that means around 50% correlation between the inhibitory activity and docking score values (Fig. S2, Supplementary data). This strongly recommends us to optimize the acridine scaffold to better understand structure activity relationship (SAR) and improve its biological activity.

In our docking study, the compounds are docked in non-covalent manner (Fig. S1, Supplementary data). Thus, it is expected that covalent binder shows weaker binding affinity such as compound **17b** (Fig. 5c); the most active inhibitor of our synthesized molecules. The branched R chain might facilitate its insertion deeply in the hydrophobic-aromatic groove. And, this might clarify its highest *in vitro* activity. As mentioned before, the flexibility of R chain increases the binding interaction in DPP-IV binding domain such as compound **2**.

Table 2. Induced fit docking (IFD) scores (Kcal/mol) and H-bond with key binding residues.

Compound	Docking scores	H-bond residues
Gemifloxacin	-8.50	Gly632-Trp629-Lys554-Glu205-Glu206
1	-8.22	Tyr662-Glu206-Glu205
2	-9.88	Tyr631-Glu206-Glu205
3	-7.43	Tyr670-Glu206-Tyr631
4	-8.10	Tyr547
5	-7.65	Tyr547-Ser630-Glu206
6	-6.95	-
7	-7.99	Tyr585-Tyr547-Tyr662-Glu205-Glu206
8	-8.21	Glu205-Ser209
9	-8.96	Lys554-Trp629-Glu206-Arg125-Glu205-Asn710
10	-8.55	Glu205-Arg125-Asn710-Lys554-Tyr547
13	-8.42	(His) Hid740-Glu206
15	-7.42	Tyr752-Asn562-Tyr547-Tyr631
17a	-7.00	Glu206-Tyr631
17b	-5.87	Lys554
17c	-7.91	Glu206-Ser630
17d	-7.62	Tyr547-Glu206-His547
17e	-7.55	Ser630-Tyr547
17f	-8.83	Asp545-Tyr547-Glu206-Arg125

Chemistry:

7-Ethoxyacridine-3,9-diamine **11** was alkylated using either acetic acid-2-chloro-2-oxoethyl ester or propanoic acid-3-chloro-3-oxoethyl ester to produce intermediates **12** and **14,** respectively. Afterward, these ester intermediates were hydrolyzed with aqueous NaOH to produce their corresponding acids **13** and **15** as shown in Scheme **1**.

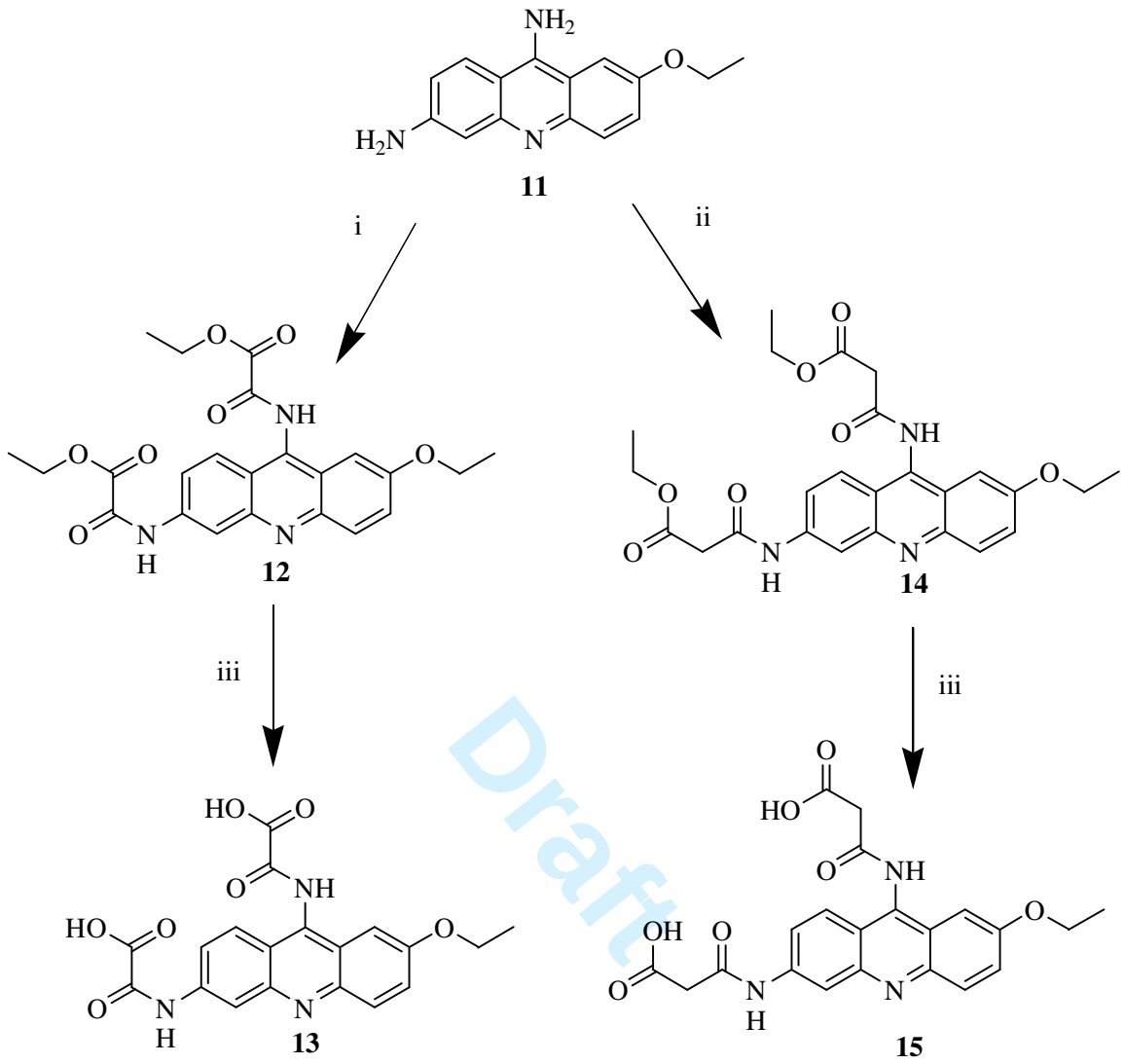

Scheme 1: Synthesis of *N*-[2-ethoxy-6-(oxalylamino)-acridin-9-yl]-oxalamic acid **13** and *N*-[6-(2-carboxy-acetylamino)-2-ethoxyacridin-9-yl]-malonamic acid **15**. Reagents: (**i**) Acetic acid-2-chloro-2-oxoethyl ester/ toluene , (**ii**) propanoic acid-3-chloro-3-oxoethyl ester, (**iii**) 1. NaOH, 2. HCl.

Furthermore, 7-ethoxyacridine-3,9-diamine **11** was alkylated using bromo acetyl chloride to produce the intermediate 2-bromo-*N*-[6-(2-bromo-acetylamino)-2-ethoxy-acridin-9-yl]-acetamide **16**. Then the bromine was displaced with a variety of appropriate amines (methanamine, *N*-methylethanamine, pyrrolidine, piperazine, piperidine and guanidine) to produce the target compounds *N*-[2-ethoxy-6-(2-(substituted-amino-acetylamino)-

acridin-9-yl]-2-(substituted-amino)-acetamide **17a**-**17f** as shown in Scheme **2** *via* nucleophilic substitution reaction.

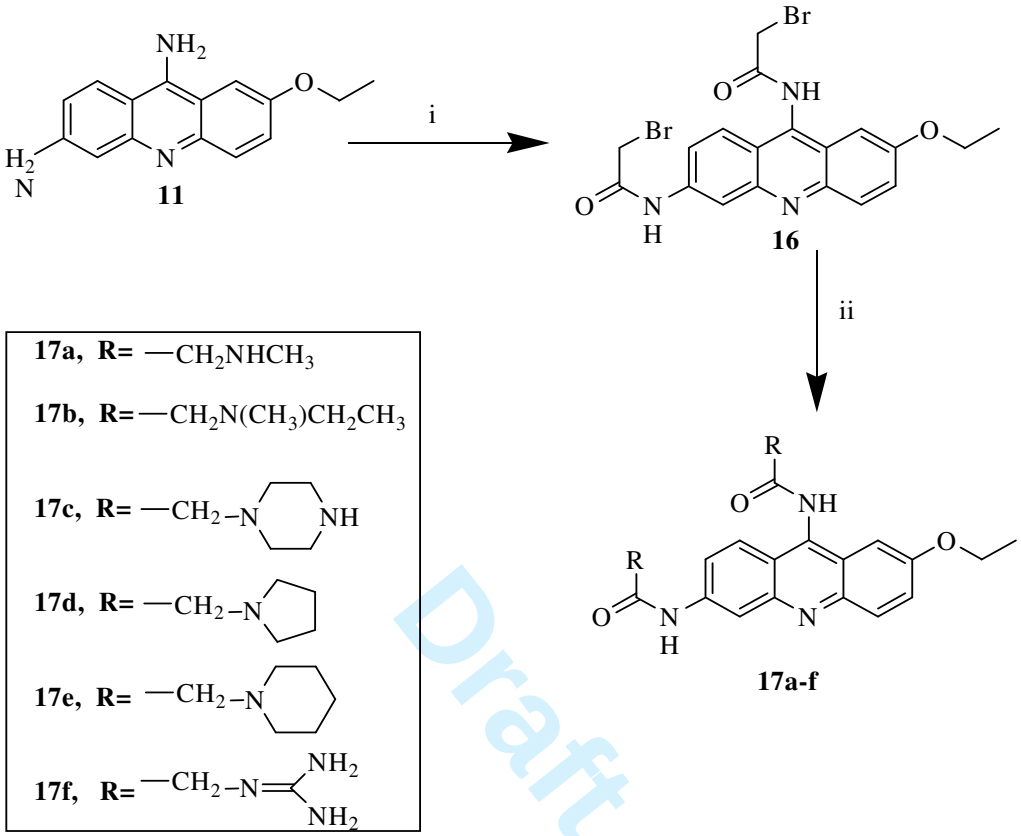

Scheme 2: Synthesis of *N*-[2-ethoxy-6-(2-(substituted-amino-acetylamino)-acridin-9-yl]-2-(substituted-amino)-acetamide **17a**-**17f**. Reagents: (**i**) Bromo acetyl chloride/ toluene, (**ii**) methanamine, guanidine, pyrrolidine, piperazine, piperidine and *N*-methylethanamine / NaI, ethanol, DMF.

The synthesized compounds were produced in yields ranging from 44% to 66.6%, with compound **15** having the highest yield.

Biological evaluation of the synthesized compounds:

Compounds **13, 15, 17a**-**17f** were tested against DPP-IV enzyme and found to exhibit anti-DPP-IV activity ranging from 2.5% to 43.8% at 30 μM concentrations. Compound

17b displayed the best activity, compounds **17c** and **17d** have moderate activities while compounds **13, 15, 17a, 17e** and **17f** have lower activities (Table 3).

Table 3. The synthesized compounds (**13**, **15**, **17a**-**17f**) rmsd values, docking scores and *in vitro* DPP-IV bioactivities.

Compound[a]	*In vitro* % inhibition of DPP-IV at 30 µM[b]	Rmsd[c]	Docking scores
13	14.7 ± 1.60	0.6	-8.4
15	12.1 ± 0.07	0.5	-7.4
17a	15.3 ± 0.92	0.5	-7.0
17b	43.8 ± 1.01	0.5	-5.9
17c	21.4 ± 1.86	0.5	-7.9
17d	28.5 ± 1.75	0.5	-7.6
17e	2.5 ± 1.48	0.5	-7.5
17f	7.3 ± 0.61	0.5	-8.8
Gemifloxacin	86.8 ± 0.47	0.6	-8.5

[a] Compounds numbers as in Schemes **1** and **2**.
[b] Values are mean ± SD
[c] Root-mean-square deviation

From Table 3, compound **13** has slightly higher activity than **15** which may indicate the effect of shortening the chain length separating the carboxylic acid group from the amide moiety.

Regarding the synthesized compounds **17a**-**17f**, it was found that compound **17b**, bearing the tertiary methylethylamine moiety as the positive ionizable feature, has the optimum activity. Presence of primary or secondary amine side chains as in compounds **17f** and **17a**, respectively reduces the anti DPP IV activity.

On the other hand, compounds enduring tertiary amine substitutions bulkier than methylethyl amine have less activity as can be seen in compounds **17c**-**17e**.

Conclusion

In conclusion, we have successfully accomplished pharmacophoric, docking and synthetic investigations of a new series of novel 2-ethoxy-6, 9-disubstituted acridine derivatives as potential DPP-IV inhibitors. It was found that incorporating acridine scaffold could be a promising approach for producing new DPP-IV inhibitors.

Moreover, it was found that the size of the backbone and the attached groups along with the ionic interaction are essential requirements for DPP-IV inhibitors. Our synthesized compounds show comparable binding affinities to the reported inhibitors and thus suggest their likelihood to be further optimized for better activities.

Conflict of interest

The authors confirm that this article content has no conflicts of interest.

Acknowledgments

We are grateful to the Scientific Research and Postgraduate Deanship at Al-Zaytoonah University of Jordan for sponsoring this project.

References

(1) Havale, S. H.; Pal, M. *Bioorg. Med. Chem.* **2009**, *17*, 1783.

(2) American Diabetes Association. *Diabetes Care* **2012**, *35*, 64.

(3) Kim, W.; Egan, J. M. *Pharmacol. Rev.* **2008**, *60*, 470.

(4) Baggio, L. L.; Drucker, D. J. *Gastroenterol*. **2007**, *132*, 2131.

(5) Edmondson, S. D.; Wei, L.; Xu, J.; Shang, J.; Xu, S.; Pang, J.; Chaudhary, A.; Dean, D. C.; He, H.; Leiting, B.; Lyons, K. A.; Patel, R. A.; Patel, S. B.; Scapin, G.; Wu, J. K.; Beconi, M. G.; Thornberry, N. A.; Weber, A. E. *Bioorg. Med. Chem. Lett.* **2008**, *18*, 2409.

(6) Gautier, J. F.; Choukem, S. P.; Girard, J. *Diabetes Metab.* **2008**, *34*, 65.

(7) Aertgeerts, K.; Ye, S.; Tennant, M. G.; Michelle, K. L.; Rogers, J.; Sang, B.; Skene, R. J.; Webb, D. R.; Prasad S. *Prot. Sci.* **2004**, *13*, 412.

(8) Gorrell, D. M.; Gysbers, V.; Mccaughan, W. G. *Scand. J. Immunol.* **2001**, *54*, 249.

(9) Kirby, M.; Yu, D.; O'connor, S.; Gorrell, M. *Clin. Sci.* (Lond) **2010**, *118*, 31.

(10) Engel, M.; Hoffmann, T.; Wagner, L.; Wermann, M.; Heiser, U.; Kiefersauer, R.; Huber, R.; Bode, W.; Demuth, H.; Brandstetter H. *PNAS* **2003**, *100*, 5063.

(11) Metzler, J.; Yanchunas, J.; Weigelt, C.; Kish, K.; Klei, H. E.; Xie, D.; Zhang, Y.; Corbett, M.; Tamura, J. K.; He, B.; Hamann, L. G.; Kirby, M. S.; Marcinkeviciene, J. *Prot. Sci.* **2008**, *17*, 240.

(12) Guasch, L.; Ojeda, J. M.; Gonzalez-Abuin, N.; Sala, E.; Cereto-Massague, A.; Mulero, M.; Valls, C.; Pinent, M.; Ardevol, A.; Garcia-Vallve, S.; Pujadas, G. *PLOS ONE* **2012**, *7*(9), e44971.

(13) Abu khalaf, R.; Abu Sheikha, G.; Al-Sha'er, M.; Taha, M. *Open Med. Chem. J.* **2013**, *7*, 39.

(14) Yin, J.; Zhu, H. U.S. Patent CN 102,675,316, A **2012**.

(15) Schoenafinger, K.; Jaehne, G.; Defossa, E.; Buning, C.; Tschank, G.; Werner, U. U.S. Patent WO 2006,018,117, A1 **2006**.

(16) Clark, R.; Kira, K.; Uehara, T.; Yoshikawa, S. U.S. Patent WO 2004,050,656, A1 **2004**.

(17) Rasmussen, K. G.; Nygaard, L.; Jensen, A. F. U.S. Patent WO 2004,033,455 A3 **2004**.

(18) Maier, R.; Himmelsbach, F.; Eckhardt, M.; Langkopf, E. U.S. Patent 7,569,574 **2004**.

(19) Schoenafinger, K.; Jaehne, G.; Defossa, E.; Billen G.; Tschank, G.; Werner, U. U.S. Patent WO 2006,015,691, A1 **2006**.

(20) Schoenafinger, K.; Jaehne, G.; Defossa, E.; Schwink, L.; Wagner, H.; Buning, C.; Tschank, G. U.S. Patent WO 2006,015,701, A1 **2006**.

(21) Himmelsbach, F.; Langkopf, E.; Eckhardt, M.; Tadayyon, M.; Thomas, L. U.S. Patent WO 2005,085,246, A1 **2005**.

(22) Nakahira, H. J.P. Patent 2003.300,977 **2003**.

(23) Baeschlin, K. D.; Clark, E. D.; Dunsdon, J. S.; Fenton, G.; Fillmore, A.; Victor, N. H., Higgs, C.; Hurley, C. A.; Krintel, S. L.; Mackenzie, R. E.; Ostermann, N.; Sirockin, F.; Sutton, M. J. U.S. Patent WO 2007,071,738, A1 **2007**.

(24) Maezaki, H.; Banno, Y.; Miyamoto, Y.; Moritou, Y.; Asakawa, T.; Kataoka, O.; Takeuchi, K.; Suzuki, N.; Ikedo, K.; Kosaka, T.; Sasaki, M.; Tsubotani, S.; Tani, A.; Funami, M.; Yamamoto, Y.; Tawada, M.; Aertgeerts, K.; Yano, J.; Oi, S. *Bioorg. Med. Chem. Lett.* **2011**, *19*, 4482.

(25) Miyamoto, Y.; Banno, Y.; Yamashita, T.; Fujimoto, T.; Oi, S.; Moritoh, Y.; Asakawa, T.; Kataoka, O.; Yashiro, H.; Takeuchi, K.; Suzuk, N.; Ikedo, K.; Kosaka, T.; Tsubotani, S.; Tani, A.; Sasaki, M.; Funami, M.; Amano, M.; Yamamoto, Y.; Aertgeerts, K.; Yano, J.; Maezaki, H. *J. Med. Chem.* **2011**, *3*, 831.

(26) Boehringer, M.; Loeffler, M. B.; Peters, J.; Riemer, C.; Weiss, P. U.S. Patent WO 2003,068,748, A1 **2003**.

(27) Burnett, D. A.; Cole D.; Domalski, M.; Josien, H.; Pissarnitski, D. A.; Sasikumar, T.; Wu, W.; Zhao Z. U.S. Patent WO 2012,078,448, A1 **2012**.

(28) Xu, F.; Corley, E.; Zacuto, M.; Conlon, D. A.; Pipik, B.; Humphrey, G.; Murry, J.; Tschaen, D. *J. Org. Chem.* **2010**, *5*, 1343.

(29) Wen-Lian, W. U.S. Patent WO 2013,006,526, A2 **2012**.

(30) Sedo, A.; Malik, R.; Vicar, J.; Simanek, V.; Ulrichov, J. *Physiol. Res.* **2003**, *52*, 367.

(31) Sutton, J. M.; Clark, D. E.; Dunsdon, S. J.; Fenton, G.; Fillmore, A.; Harris, N. V.; Higgs, C.; Hurley, C. A.; Krintel, S. L.; MacKenzie, R. E.; Duttaroy, A.; Gangl, E.; Maniara, W.; Sedrani, R.; Namoto, K.; Ostermann, N.; Gerhartz, B.; Sirockin, F.; Trappe, J.; Hassiepen, U.; Baeschlin, D. K. *Bioorg. Med. Chem. Lett.* **2012**, *22*, 1464.

(32) Protein Preparation Wizard, Maestro, MacroModel, Phase, Induced Fit, Jaguar, and Glide; Schrödinger, LLC: Portland, OR, **2009**.

(33) Edmondson, S. D.; Wei, L.; Xu, J.; Shang, J.; Xu, S.; Pang, J.; Chaudhary, A.; Dean, D. C.; He, H.; Leiting, B.; Lyons, K. A.; Patel, R. A.; Patel, S. B.; Scapin, G.; Wu, J. K.; Beconi, M. G.; Thornberry, N. A.; Weber, A. E. *Bioorg. Med. Chem. Lett.* **2008,** *18*, 2409.

(34) Edmondson, S. D.; Mastracchio, A.; Cox, J. M.; Eiermann, G. J.; He, H.; Lyons, K. A.; Patel, R. A.; Patel, S. B.; Petrov, A.; Scapin, G.; Wu, J. K.; Xu, S.; Zhu, B.; Thornberry, N. A.; Roy, R. S.; Weber, A. E. *Bioorg. Med. Chem. Lett.* **2009**, *15*, 4097.

(35) Yoshida, T.; Akahoshi, F.; Sakashita, H.; Sonda, S.; Takeuchi, M.; Tanaka, Y.; Nabeno, M.; Kishida, H.; Miyaguchi, I.; Hayashi, Y. *Bioorg. Med. Chem.* **2012**, *16*, 5033.

(36) Wallace, M. B.; Feng, J.; Zhang, Z.; Skene, R. J.; Shi, L.; Caster, C. L.; Kassel, D. B.; Xu, R.; Gwaltney, S. L. *Bioorg. Med. Chem. Lett.* **2008**, *7*, 2362.

(37) Goda, F.; Abdel-Aziz, A.; Ghoneim, H. *Bioorg. Med. Chem*. **2005**, *13*, 3175.

(38) Neidle, S.; Harrison, J.; Kelland, L.; Gowan, S.; Read, M.; Reskza, A. U.S. Patent 7,160,896, B2 **2007**.

(39) Samuels, Y.; Diaz, L. A.; Schmidt-Kittler, O.; Cummins, J. M.; DeLong, L.; Cheong, I.; Rago, C.; Huso, D. L.; Lengauer, C.; Kinzler, K. W.; Vogelstein, B.; Velculescu, V. E. *Cancer Cell* **2005**, *7*, 561.

(40) Sherman, W.; Beard, H. S.; Farid, R. *Chem. Biol. Drug Des.* **2006**, *67*, 83.

(41) Sherman, W.; Day, T.; Jacobson, M. P.; Friesner, R. A.; Farid, R. *J. Med. Chem.* **2006**, *49*, 534.

(42) Friesner, R. A.; Banks, J. L.; Murphy, R. B.; Halgren, T. A.; Klicic, J. J.; Mainz, D. T.; Repasky, M. P.; Knoll, E. H.; Shelley, M.; Perry, J. K.; Shaw, D. E.; Francis, P.; Shenkin, P. S. *J. Med. Chem.* **2004**, *47*(7), 1739.

(43) Friesner, R. A.; Murphy, R. B.; Repasky, M. P.; Frye, L. L.; Greenwood, J. R.; Halgren, T. A.; Sanschagrin, P. C.; Mainz, D. T. *J. Med. Chem.* **2006**, *49*, 6177.

Supplementary data

Fig. S1. Synthesized compounds (**13**, **15**, **17a-17f**) mapped against the pharmacophore model and docked within DPP-IV binding site.

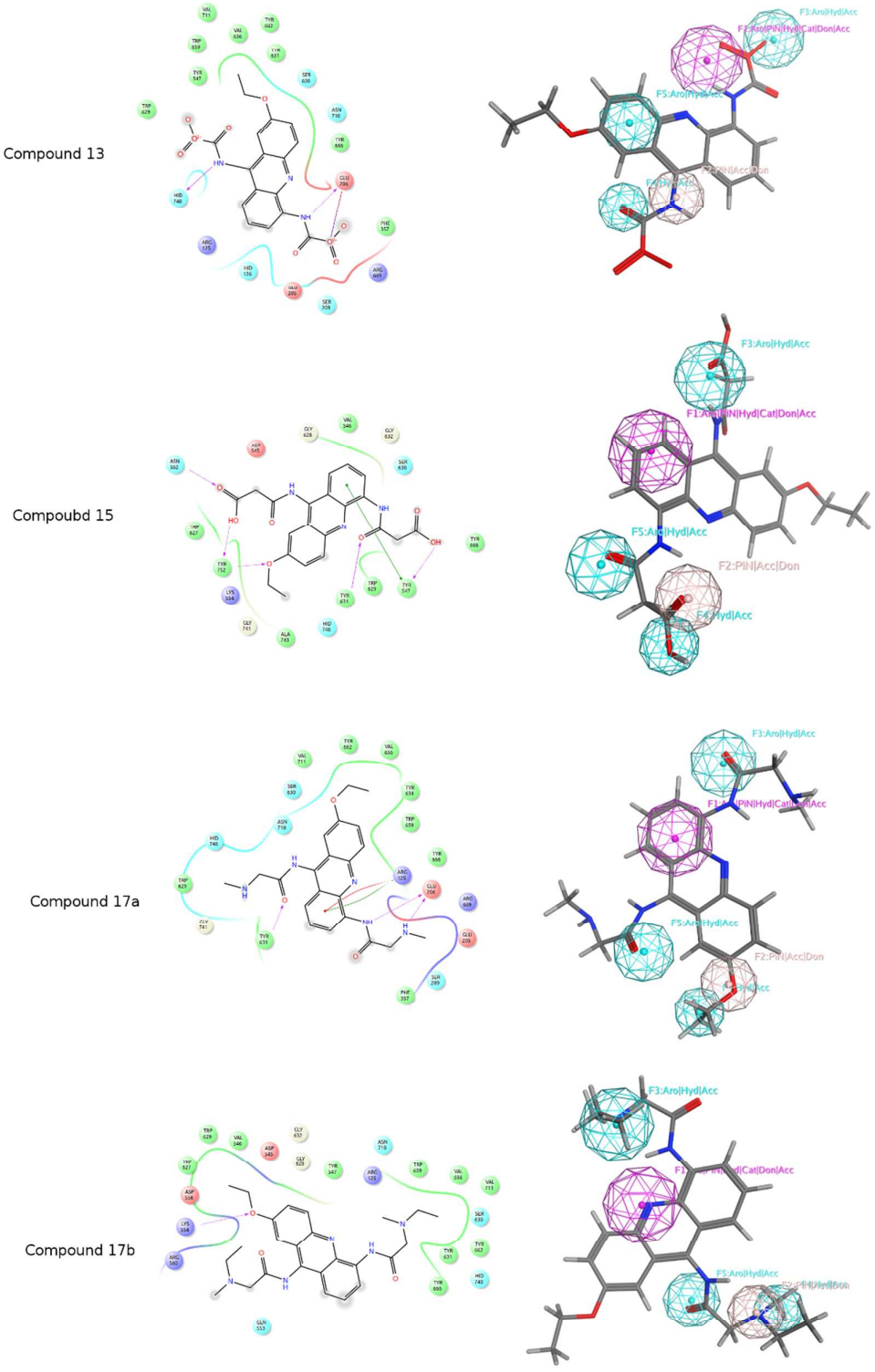

Compound 17c

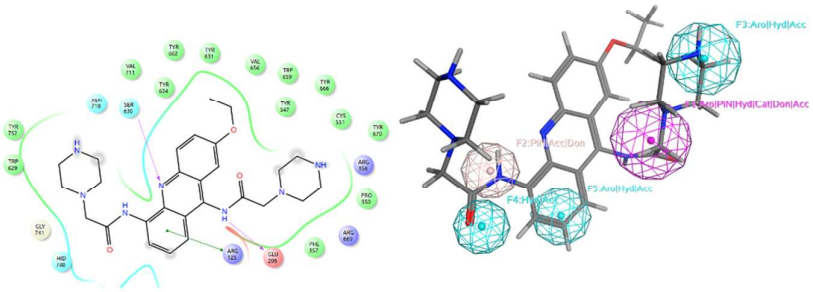

Compound 17d

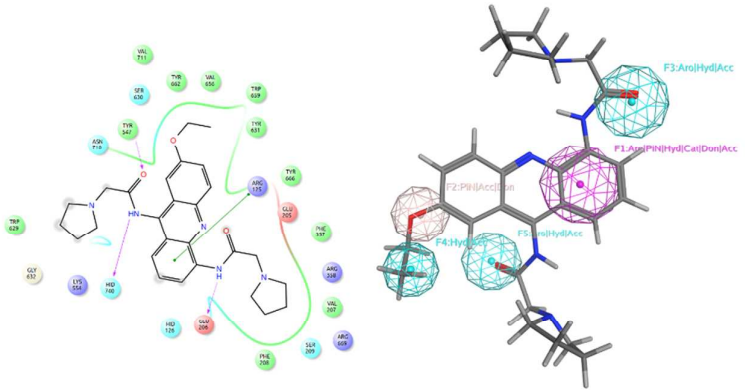

Compound 17e

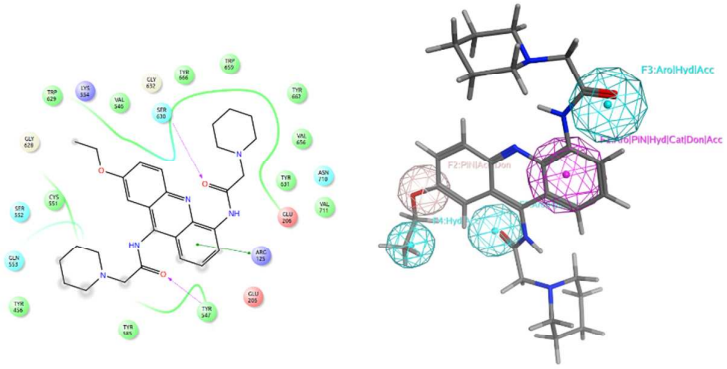

Compound 17f

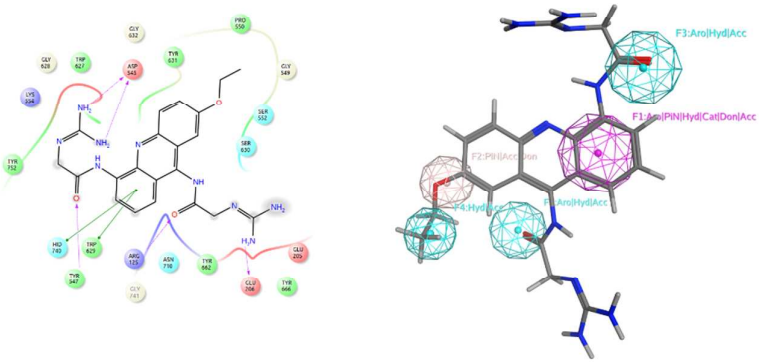

Fig. S2. The % inhibition versus IFD docking scores (Kcal/mol).

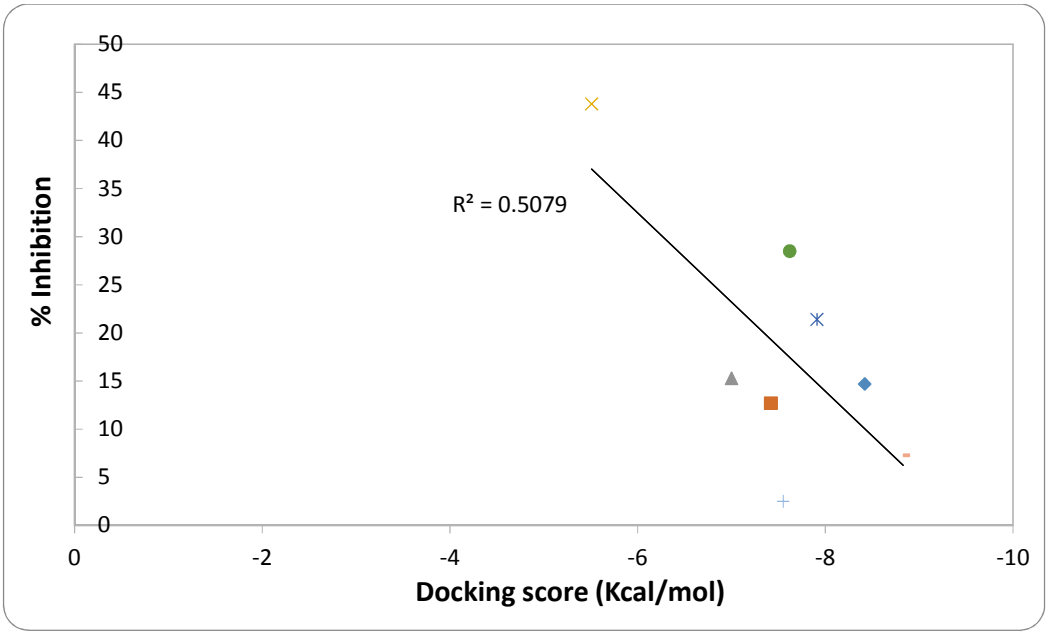

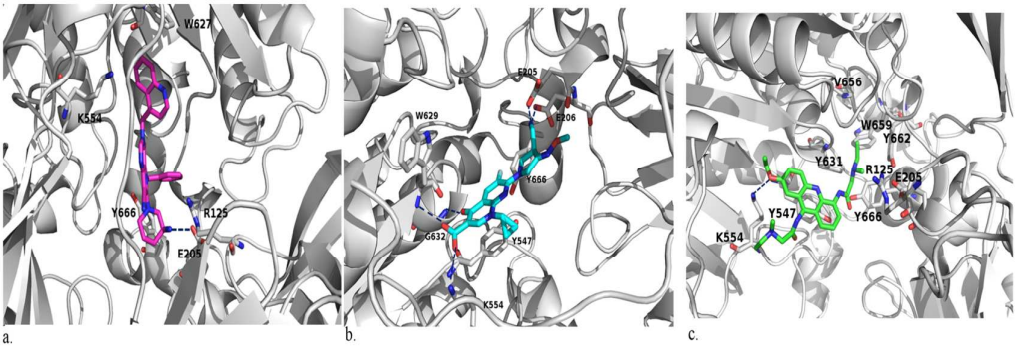
W627
K554
Y666
R125
E205
a.
E205
E206
W629
Y666
G632
Y547
K554
b.
V656
W659
Y662
Y631
R125
E205
Y547
Y666
K554
c.